J. Phys. B: At. Mol. Opt. Phys. **33** (2000) 507–520. Printed in the UK PII: S0953-4075(00)07974-8

Spatially periodic structures in electron swarms and the Franck–Hertz experiment

R E Robson, B Li and R D White

School of Mathematics and Physics, James Cook University, Cairns 4870, Australia

Received 17 September 1999, in final form 9 November 1999

Abstract. The seminal experiment of Franck and Hertz, which helped lay the foundations of quantum and atomic physics, is investigated through solution of the Boltzmann equation, using both eigenfunction expansion methods and spatial finite-difference techniques. We consider electrons in both a model gas and in mercury, the gas originally used by Franck and Hertz, and focus upon the effects of both inelastic and elastic collisions. It is pointed out that the periodic spatial structures encountered in the Franck–Hertz experiment have a physical origin similar to the oscillatory phenomena observed by Fletcher and others previously in low-pressure, low-current discharges, and by Winkler *et al*, and other contemporary authors in simulations of low-temperature plasmas.

1. Introduction

The seminal experiment of Franck and Hertz [1] confirmed the Bohr quantization postulates and helped lay the foundations of modern atomic theory. For present purposes, it may be represented schematically as in figure 1. Here a source emits electrons at a steady rate into a gas occupying the region between two plane-parallel electrodes, there being a control grid in front of the anode, which allows through only those electrons with energies in excess of a certain value.

The current I_c collected by the anode is observed to go through successive maxima and minima as the applied voltage U increases, the 'period' ΔU of the fluctuations being related to the threshold energy ε_I for excitation of the gas atom by inelastic collisions through $e\Delta U = \varepsilon_I$, according to the usual textbook arguments. For mercury gas as originally used by Franck and Hertz, $e\Delta U$ is observed to be close to the threshold energy of 4.89 eV for the $6\ ^1S_0 \rightarrow 6\ ^3P_1$ transition. The textbook picture of the physical situation is one of an electron being successively accelerated by the electric field $E = U/d$ and brought abruptly to rest when it has sufficient energy to undergo an inelastic collision with the gas atom. The mean electron energy thus fluctuates downstream from the source, with the spatial period $\Delta z = \varepsilon_I/eE$. It is this periodic spatial structure which is the focus of attention in the present paper.

While the above argument explains the broad features of the Franck–Hertz experiment and certainly gets to the essence of quantization of atomic states, it is nevertheless far from complete from both an atomic physics and a kinetic theory point of view, a fact which has been highlighted by Hanne [2]. In the textbook arguments, the electrons are discussed as if they formed a monoenergetic beam, while Hanne simply assumes a Maxwellian distribution of velocities, and neglects elastic collisions. McMahon [3] devoted an article to the effect of elastic collisions in the Franck–Hertz experiment, albeit in a rather heuristic way. Given that

0953-4075/00/030507+14$30.00

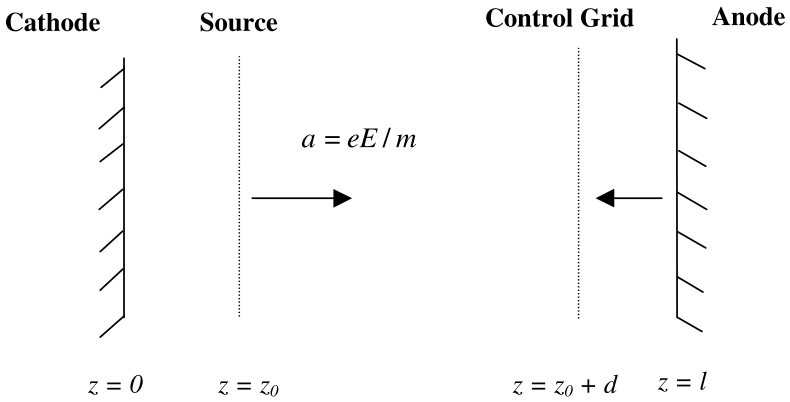

Figure 1. Schematic representation of the Franck–Hertz experiment, showing a steady source at $z = z_0$ (usually at the cathode, i.e. $z_0 = 0$) emitting electrons into a gas occupying the space between two plane-parallel electrodes, subject to a uniform electric field E. The control grid at distance d and at potential $U = Ed$ downstream from the source allows only electrons above a certain energy to be collected by the anode.

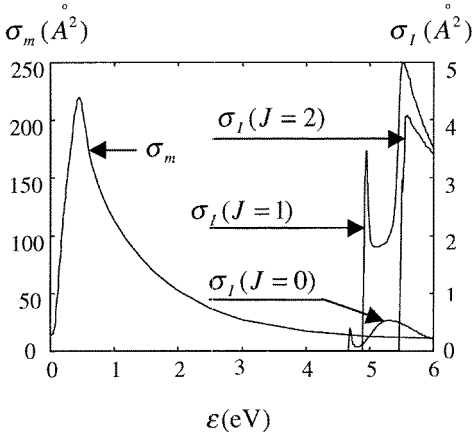

Figure 2. The momentum transfer cross section σ_m and three inelastic cross sections σ_I for electron scattering from mercury [2, 4].

the momentum transfer cross section for mercury atoms is enormous [4], as shown in figure 2, it is clear that elastic scattering must be taken seriously in any sophisticated analysis.

We feel that a rigorous analysis of the Franck–Hertz experiment in the context of modern kinetic theory is long overdue, and the present paper takes the first steps in this direction.

Besides an intrinsic interest in the problem, we are also motivated by the following considerations:

(a) The arrangement in figure 1 can be thought of as a type of steady-state Townsend 'swarm' experiment, and as such, contact can usefully be made with the swarm physics literature. There the conventional view is that properties simply decay monotonically to equilibrium downstream from the source, and the spatial dependence is governed by the 'hydrodynamic' regime. However, Fletcher [5] has pointed out that periodic structures in low-current, low-pressure discharges have long been known [6–9], dating back almost

to the days of Franck and Hertz. Fletcher himself employed the photon flux technique in measurements of electron transport properties in several noble gases at low pressure, and observed a damped periodic dependence consistent with the Franck–Hertz experiment. He showed that the oscillations could be quenched through addition of only a few per cent molecular gas admixture, deducing that unless there exists a large gap between the ground state and the first excited states, properties downstream from the source will simply decay monotonically to equilibrium.

(b) There is a large and growing body of modern literature [10–17] dealing with spatial inhomogeneities in low-temperature plasmas, in which damped periodic structures have been reported. The group led by Winkler [12–14] has demonstrated pronounced sensitivity to E/n_0 (the ratio of the field to the gas number density), and shown that it is only at *intermediate* fields that periodicity is observed. The explanation given in [14] essentially follows the classical Franck–Hertz argument and confirms Fletcher's suggestion [5] that increasing the number of inelastic channels enhances damping. Reference [14] is particularly noteworthy for introducing a 'multiterm' analysis of Boltzmann's equation capable of dealing with spatial inhomogeneities, in contrast to the severe limitations which many authors place on their work by unnecessarily limiting the representation of the electron velocity distribution function to the first two terms of an expansion in spherical harmonics. It is to be emphasized that while Winkler *et al* and others go on to deal with inhomogeneous fields and space-charge phenomena, this is not in any way connected with the effects we are presently discussing.

(c) Returning to swarm theory *per se*, a modern view [18] is that *all* swarm experiments can be analysed from a common standpoint, in which a generalized eigenvalue equation, and an associated 'dispersion relation', furnish all quantities of physical interest. If, as we argue, the Franck–Hertz experiment can be thought of as belonging to the steady-state Townsend category, then the full weight of modern eigenvalue theory [18, 19] can be brought to bear. This is most useful for dealing with the asymptotic region far downstream from the source, where the eigenvalue with the lowest real part controls the spatial structure. A comprehensive analysis is given by Li [20], and results are summarized in what follows.

It is evident that in revisiting the classic Franck–Hertz experiment we can profitably link together several seemingly disparate strands of the literature, both modern and traditional, and at the same time discuss some very rich and interesting phenomena.

In section 2 we review kinetic eigenvalue theory in the context of the present problem and provide calculations for simple cross section models. In section 3, we consider mercury gas, both from the point of view of an eigenfunction expansion and using a spatial finite-difference method. Our aim is to use a multiterm representation in velocity space in all cases, to avoid the limitations of the two-term theory as described above.

2. Kinetic theory and model gas calculations

2.1. Formal kinetic theory

The aim of this section is to develop a kinetic theory appropriate for dealing with spatially inhomogeneous electron swarms in spatially uniform electric fields. Such swarm particles interact with the gas molecules and atoms filling the chamber, but not with each other, and do not disturb significantly the overall equilibrium of the gas, or distort the applied field. This is the 'test particle' problem of plasma physics by a different name. Such conditions are realized experimentally by limiting sources to low currents. The great theoretical simplification associated with swarms is that the Boltzmann kinetic equation is *linear* in the phase space

distribution function. For steady-state conditions and the plane-parallel geometry of figure 1, it can be written quite generally as

$$(M + c_z\partial/\partial z) f(z, \boldsymbol{c}) = S(\boldsymbol{c})\delta(z - z_0) \tag{1}$$

where

$$M = J + a_z\partial/\partial c_z. \tag{2}$$

J is the linear collision operator describing electron–gas molecule interactions (elastic, inelastic, ionizing, attaching), $a_z = -eE_z/m$ is the acceleration experienced by an electron under the influence of an electrostatic field E_z (an accelerating field of magnitude E and directed in the $-z$-direction between $z = z_0$ and $z = z_0 + d$, and a retarding field of a different magnitude and directed in the $+z$-direction between $z = z_0 + d$ and $z = l$), $f(z, \boldsymbol{c})$ is the phase space distribution function, and $S(\boldsymbol{c})$ represents the rate of production of electrons with velocities $\boldsymbol{c}$ by the source. The problem is completed by specifying the boundary conditions on f at the electrodes. The quantity determined experimentally is the current collected by the anode,

$$I_c = e\int \mathrm{d}\boldsymbol{c}\, c_z f(l, \boldsymbol{c}) \tag{3}$$

which can be calculated once the solution of (1) is available. Given that E_z is inhomogeneous, reversing the sign at $z = z_0 + d$ in the picture shown in figure 1, obtaining f from (1) is quite a formidable problem.

So much for the formal, rigorous picture. It is not usually posed in this way, but it is just as well to recognize what is really involved in an analysis of the actual Franck–Hertz experiment. To make any further progress, we elect to make some simplifications. Thus, it is assumed that the whole drift region is occupied by a uniform field E in the $-z$-direction, resulting in a uniform acceleration

$$a_z = a = -eE/m \tag{4}$$

everywhere. The role of the gate now merely acts in a non-perturbing way to 'label' high-energy electrons for subsequent sampling, the current measured in experiment now being approximated by

$$I_c = e\int_{c_z > c_{\min}} \mathrm{d}\boldsymbol{c}\, c_z f(z_0 + d, \boldsymbol{c}) \tag{5}$$

the integral now being over velocities for which c_z exceeds some critical cut-off value $c_{\min}$.

Furthermore, boundary conditions are not imposed, or rather, the anode is pushed away to infinity, i.e. $l \to \infty$. Thus, equation (1) is solved on the infinite half-plane $z_0 < z < \infty$, with the only constraint being that f must remain finite as $z \to \infty$.

In effect, we have reduced the Franck–Hertz experiment to an equivalent steady-state Townsend experiment, thereby allowing us to bring to bear much of the modern kinetic theory of swarms [18, 19].

2.2. Solution in terms of eigenvalues and eigenfunctions

The solution of (1) downstream from the source ($z > z_0$) can be written as

$$f(z, \boldsymbol{c}) = \sum_{j=0}^{\infty} \exp[K_j(z - z_0)]\, \psi_j(\boldsymbol{c}) \int S(\boldsymbol{c}_0)\, \varphi_j^*(\boldsymbol{c}_0)\, \mathrm{d}\boldsymbol{c}_0 \tag{6}$$

where K_j are the eigenvalues, with a non-positive real part, and ψ_j, φ_j are the eigenfunctions of the dual problem,

$$(M + K_j c_z)\psi_j = 0 \tag{7a}$$

$$(M^+ + K_j c_z)\varphi_j^* = 0 \tag{7b}$$

while

$$M^+ = J^+ - a_z \partial/\partial c_z \tag{8}$$

and J^+ is the adjoint of the Boltzmann collision operator. Note the orthogonality property

$$\int c_z \psi_k \varphi_j^* \, \mathrm{d}\boldsymbol{c} = \delta_{jk}. \tag{9}$$

The lowest eigenvalue and corresponding eigenfunctions are

$$K_0 = 0 \tag{10}$$

and

$$\varphi_0 = 1 \tag{11}$$

while ψ_0 is the equilibrium distribution function satisfying

$$(J + a\partial/\partial c_z)\psi_0 = 0. \tag{12}$$

The distribution function (6) and its moments tend asymptotically toward their respective equilibrium values at a rate controlled by K_1, the eigenvalue with the lowest (in magnitude) real part. This particular eigenvalue is therefore of special interest in what follows.

Note that the particle flux is given by the constant value (considering particle-conservative collisions only)

$$\Gamma = \int \mathrm{d}\boldsymbol{c}\, c_z f(z, \boldsymbol{c}) = \int \mathrm{d}\boldsymbol{c}_0 \, S(\boldsymbol{c}_0) \tag{13}$$

a fact which follows from (9) and (11), and independently of course from continuity in the steady-state condition. The leading terms of (6) are therefore

$$f(z, \boldsymbol{c}) = \Gamma\psi_0(\boldsymbol{c}) + S_1\psi_1(\boldsymbol{c}) \exp[K_1(z - z_0)] + \cdots \tag{14}$$

where

$$S_j = \int \mathrm{d}\boldsymbol{c}_0 \, S(\boldsymbol{c}_0) \, \varphi_j^*(\boldsymbol{c}_0) \qquad (j = 0, 1, 2, \ldots). \tag{15}$$

The moments of physical interest are:

Number density:

$$n(z) = \int \mathrm{d}\boldsymbol{c}\, f(z, \boldsymbol{c}) = n_\infty + n_1 \exp[K_1(z - z_0)] + \cdots. \tag{16}$$

Average velocity:

$$v(z) = \Gamma/n(z) = v_\infty/\{1 + v_1 \exp[K_1(z - z_0)] + \cdots\}. \tag{17}$$

Mean energy:

$$\varepsilon(z) = \int \mathrm{d}\boldsymbol{c}\, \tfrac{1}{2}mc^2 f(z, \boldsymbol{c})/n(z)$$
$$= \varepsilon_\infty\{1 + \varepsilon_1 \exp[K_1(z - z_0)] + \cdots\}/\{1 + v_1 \exp[K_1(z - z_0)] + \cdots\}. \tag{18}$$

In these expressions, the equilibrium moments are

$$n_\infty = \Gamma \int \mathrm{d}\boldsymbol{c}\, \psi_0(\boldsymbol{c}) \tag{19a}$$

$$v_\infty = \Gamma/n_\infty \tag{19b}$$

$$\varepsilon_\infty = \int \mathrm{d}\boldsymbol{c}\, \tfrac{1}{2}mc^2 \psi_0(\boldsymbol{c}) / \int \mathrm{d}\boldsymbol{c}\, \psi_0(\boldsymbol{c}) \tag{19c}$$

while n_1, v_1 and ε_1 are constants determined by integrals over $\psi_0(\boldsymbol{c})$ and $\psi_1(\boldsymbol{c})$.

Note that while the terms as shown in (16)–(18) determine the asymptotic behaviour in general for any source strength $S(\boldsymbol{c})$ far downstream from the source, all terms and all eigenvalues K_j $(j = 0, 1, 2, 3, \ldots)$ are generally required near the source. However, one can construct artificially a situation where only a few terms are non-zero at all positions, by assuming a source strength which is expressible as a linear combination of a few low-order eigenfunctions, e.g.

$$S(\boldsymbol{c}) = A_0\psi_0(\boldsymbol{c}) + A_1\psi_1(\boldsymbol{c}). \tag{20}$$

Then by virtue of the orthogonality relation (9), equation (15) implies that only S_0 and S_1 are non-vanishing, and therefore (6) and all subsequent expressions terminate exactly at $j = 1$ for all positions z.

2.3. Results for model gases

Numerical method and accuracy test. In general, the key equations (7*a*) and (7*b*) have to be solved numerically. The method we have used is the traditional one in the kinetic theory of gases, namely, to expand about a Maxwellian in terms of Burnett functions, at an arbitrary basis temperature [21, 22], the so-called 'two-temperature' theory of charged particle transport [23]. The operator equations (7*a*) and (7*b*) are thereby converted into an infinite set of coupled algebraic equations for the moments of the distribution function. The K_j are then simply found as the eigenvalues of this matrix, truncated to finite size. Details of the procedure, including a discussion of accuracy associated with this truncation and the choice of the basis temperature,

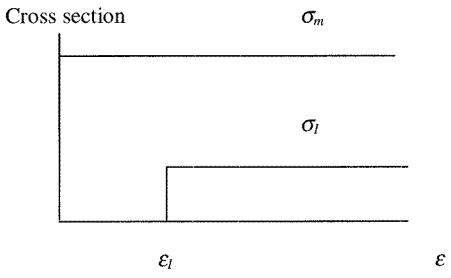

Figure 3. Cross sections for model gas calculations.

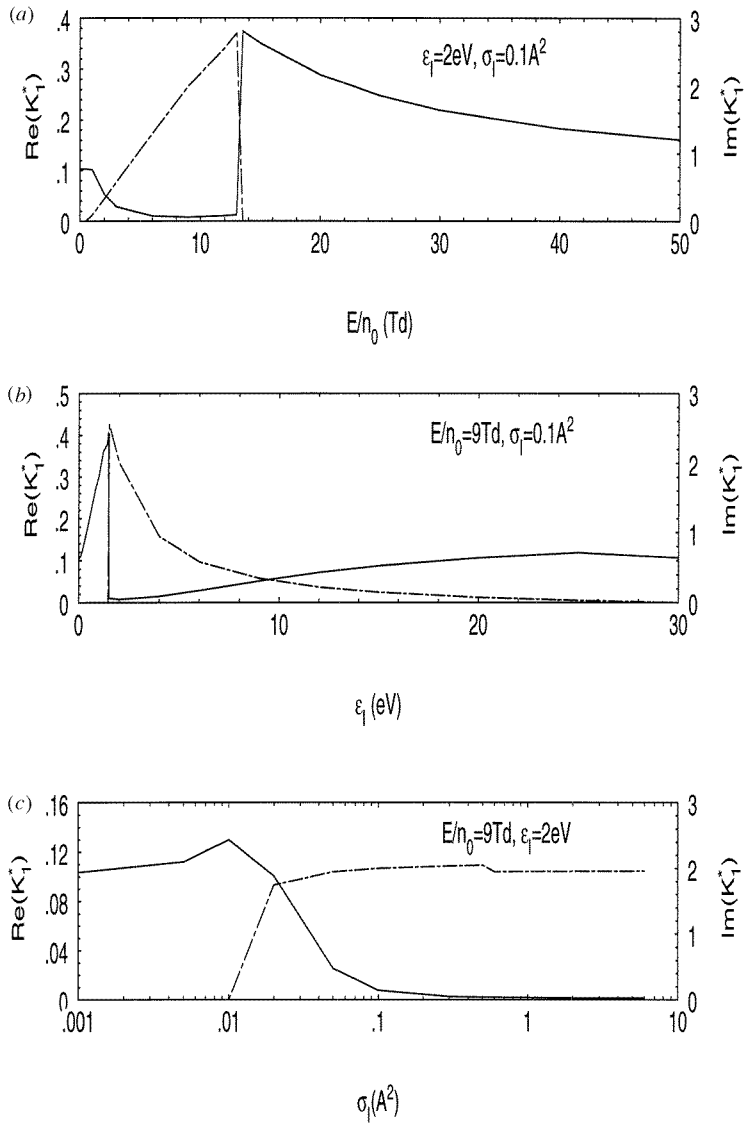

Figure 4. The (negative of the) real (full curve) and imaginary (chain curve) parts of the eigenvalue corresponding to $j = 1$ as a function of (*a*) electric field, (*b*) threshold and (*c*) inelastic cross section amplitude for the step function model. The normalized eigenvalue is $K_1^* = -K_1\lambda$, where $\lambda = (\sqrt{2}n_0\sigma_0)^{-1}$ is a constant with the dimension of length, representative of the mean free path, and $\sigma_0 = 1$ A^2.

can be found in [20]. Note, however, that we place no limitations on the number of spherical harmonics, i.e. we have a 'multiterm' theory in contemporary parlance. For the present, we note that the integrity of the computer program can be tested by comparison with the one case for which an exact analytic solution is possible, namely, when collisions are elastic and governed by a constant collision frequency ν_m. Then it can be shown that [20]

$$K_j = -2j(j+3)\alpha^2 a/(4j+3)^2 \tag{21}$$

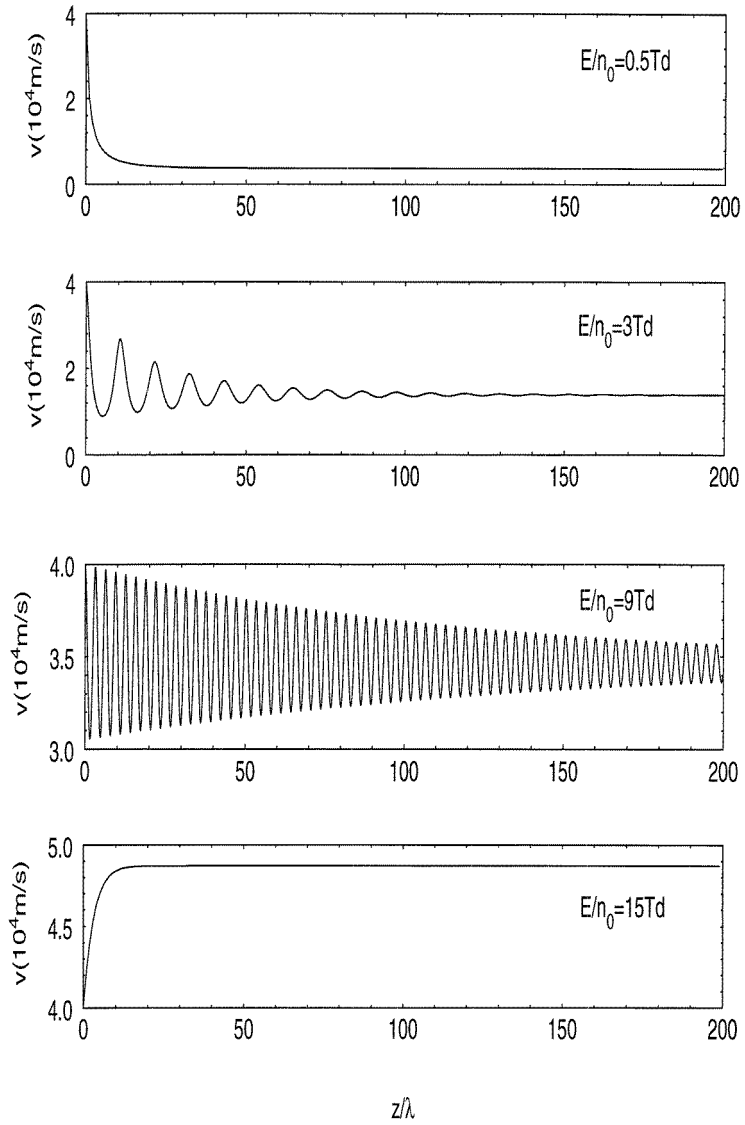

Figure 5. Spatial relaxation of average velocity for electrons in a gas governed by a step function collision model for a range of fields. Distance is normalized to λ as defined in figure 4.

where

$$\alpha^2 = 3m/m_0(\nu_m/a)^2$$

and m_0 is the mass of a neutral particle. Using this result, the accuracy of the first few eigenvalues as calculated by the Burnett function expansion techniques is found to be around 1% or better.

Step function model. We now take a model gas with constant elastic cross section and one inelastic channel, as shown in figure 3. The other parameters are $T_0 = 0$ K, $m_0 = 4$ amu and

$\sigma_m = 6$ A^2. We shall take $\sigma_m = 0.1$ A^2, $\varepsilon_I = 2$ eV, $E/n_0 = 9$ Td (1 Td = 1 Townsend = 10^{-21} V m^2) unless otherwise stipulated. Figure 4 shows the way in which the real and imaginary parts of K_1 vary with each of the parameters. We next take a source strength of the form (20), so that only the lowest two eigenvalue 'modes' are involved over the entire range of z. Figure 5 then shows how average velocity varies with position as E/n_0 changes. The mean energy exhibits similar oscillatory patterns. All these results are consistent with the observations of Fletcher [5] and Winkler and co-workers [12–14]. Specifically, we note that lightly damped oscillatory behaviour occurs only if the threshold for the inelastic process is sufficiently high, and that there is clearly a 'window' of field strengths for which it is observed.

More specific calculations reveal that the results shown in figures 4 and 5 are consistent with the traditional physical arguments made in connection with the Franck–Hertz experiment and repeated in the introduction to this paper. Thus the separation Δz between successive peaks and troughs is expected to be given by the relation $eE\Delta z = \varepsilon_I$ or equivalently in terms of the imaginary part of the eigenvalue,

$$\mathrm{Im}(K_1) = 2\pi eE/\varepsilon_I. \tag{22a}$$

The corresponding expression in terms of the dimensionless eigenvalue of figure 4 is

$$\mathrm{Im}(K_I^*) = 0.444(E/n_0)_{\mathrm{Td}}/\varepsilon_I(\mathrm{eV}). \tag{22b}$$

An examination of figure 4 shows that when K_1 is complex, $\mathrm{Im}(K_I^*)$ is indeed proportional to E/n_0 and inversely proportional to ε_I, with numerical values in accordance with (22*b*). Likewise, there is no dependence upon σ_I (above a certain threshold). Note that the sharp variation of both real and imaginary parts of K_1 can be understood through momentum transfer theory [20].

From now on, we move to calculations of more direct relevance to the Franck–Hertz experiment.

3. Studies of mercury gas

3.1. Eigenvalue method

We now employ the eigenvalue technique for electrons in mercury gas, as originally used by Franck and Hertz [1], with the England, Elford–Hanne cross sections [2, 4] as shown in figure 2. Again, the artificial source strength (20) is used to enable a complete spatial representation with only the lowest two modes. The results are shown in figures 6(*a*) and (*b*) for the mean energy and average velocity, respectively, at values of E/n_0 consistent with voltages and pressures used in the experiment. If the value of E/n_0 is such that the control grid in figure 1 coincides with a maximum (minimum) in the mean energy, the collector current versus voltage curve also has a maximum (minimum). The spacing between peaks corresponds closely (but not exactly) with the expected value of 4.9 eV.

These calculations allow for elastic collisions, whereas a traditional discussion neglects such collisions entirely, in effect setting the elastic cross section equal to zero. The last two curves in figures 6(*a*) and (*b*) show what happens when σ_m is reduced by a factor of 10 from the values shown in figure 2: the amplitude of oscillations is markedly increased, and damping is also significantly reduced. However, the 'period' is essentially unaltered and this is the key experimental quantity determined in the Franck–Hertz experiment. That is, since the experiment focuses solely on examination of the quantization of atomic levels, the neglect of elastic collisions appears justified. Of course, if one is interested in the detailed spatial structure, it is an entirely different story.

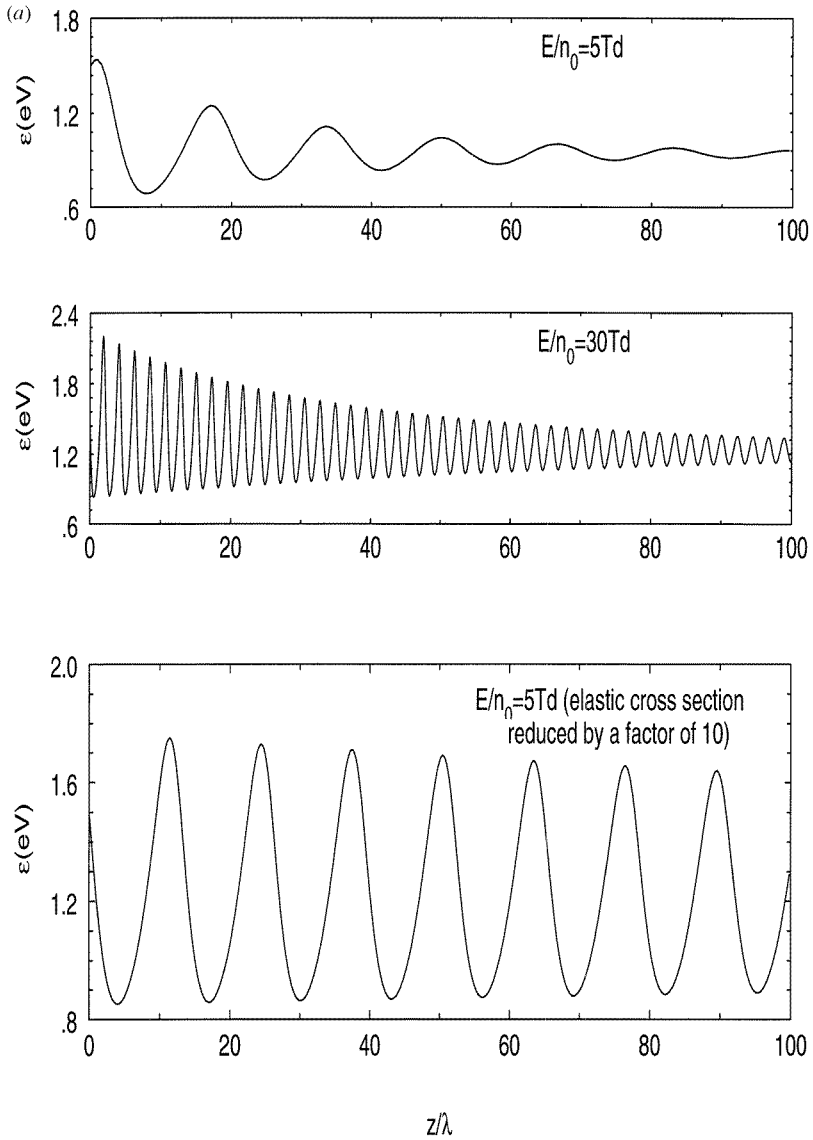

Figure 6. Spatial relaxation of (*a*) the mean energy and (*b*) the average velocity for electrons in mercury for a range of E/n_0 realized in the Franck–Hertz experiment.

In the calculations presented in this section we have constructed an artificial source to enable us to get the complete picture, both close to and far from the source, with only a few eigenvalues. In practical situations, with real sources, only the asymptotic downstream region will be described by these lowest 'modes'. Close to the source, a large number of modes will contribute and the eigenvalue approach is therefore of limited value. We therefore seek an alternative numerical technique which allows us to calculate profiles by solving (1) directly.

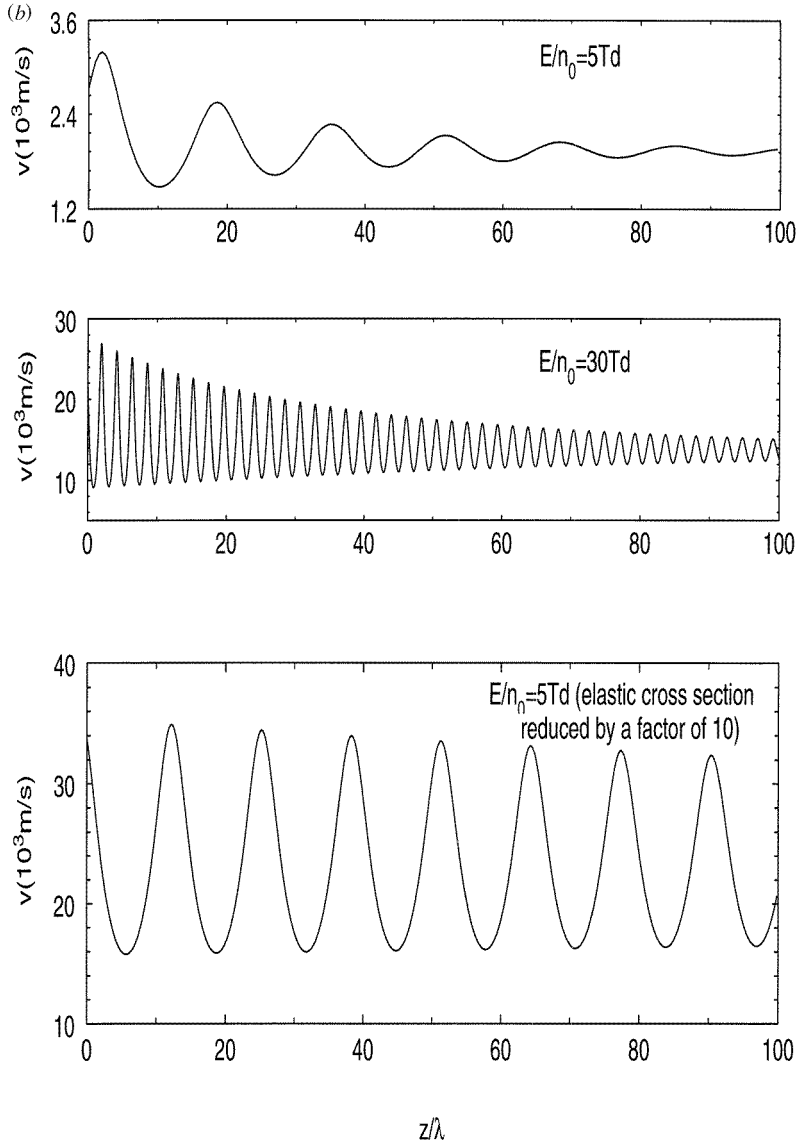

Figure 6. Continued.

3.2. Determination of the full spatial structure with finite-difference method

For the remaining calculations we choose to work with a slightly different formulation of the problem, whereby we solve the Boltzmann equation without specifying a source, i.e.

$$(M + c_z \partial/\partial z)\, f(z, \boldsymbol{c}) = 0 \tag{23}$$

but specify instead certain information about the distribution function at z_0, i.e. $f(z_0, \boldsymbol{c})$. Note, however, that there is another physical constraint at infinity, i.e. the distribution function must be finite, specifically

$$f(z, \boldsymbol{c}) \to \psi_0(\boldsymbol{c}) \qquad \text{as} \quad z \to \infty \tag{24}$$

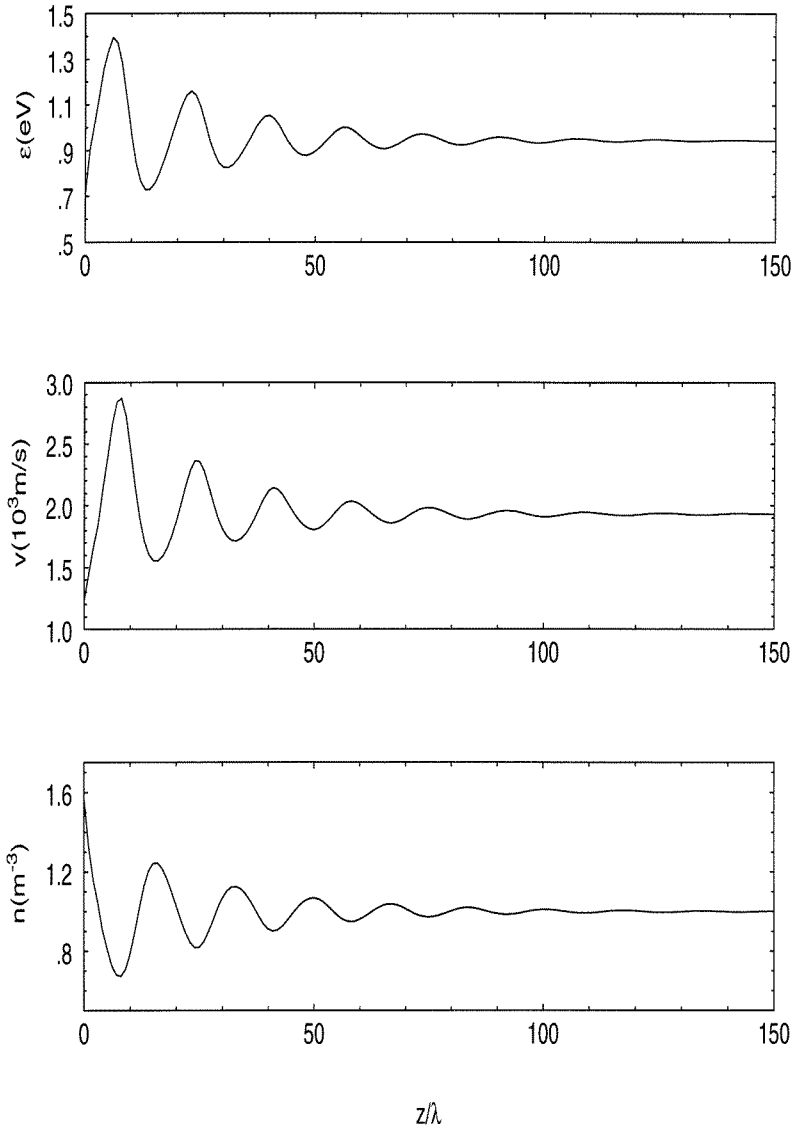

Figure 7. Relaxation profiles of the mean energy, average velocity and number density for electrons in mercury as calculated with a finite-difference method for $E/n_0 = 5$ Td.

where ψ_0 is the solution of the equilibrium Boltzmann equation (12). Note that the value of $f(z_0, \boldsymbol{c})$ must be specified only in the half-space $c_z > 0$, or equivalently, specifying only *half* the spherical harmonic expansion coefficients $f^{(l)}(z_0, \boldsymbol{c})$ with $l = 1, 3, 5, \ldots$ [24]. To do otherwise amounts to an overspecification of the boundary conditions for the problem. The numerical technique employed is an expansion in Burnett functions $\phi_m^{[v,l]}(\boldsymbol{c})$ in velocity space as before (again no limitations on the number of spherical harmonics), with a second-order finite-difference representation of the spatial derivative in (23). The number density, average velocity and mean energy profiles for electrons entering mercury gas with a speed Maxwellian velocity distribution function at mean energy 0.776 eV are shown in figure 7, where the applied

electric field is $E/n_0 = 5$ Td. To achieve a typical accuracy of a few per cent for the moments shown, we have taken terms up to $l_{\max} = 2$, $\nu_{\max} = 50$ and about 200 spatial mesh points. Here we note that, especially when a multiterm method is implemented, we are dealing with very large sets of algebraic equations (for this case, around 2×10^4), for which special computational techniques must be employed, further details can be found in [20].

With the initial conditions stated above, *all* eigenmodes now effectively contribute near the source, and therefore the profiles are consequently a bit irregular, when compared with the smooth variations depicted in figures 5 and 6, for which unrealistic initial conditions were effectively imposed to eliminate all but the lowest modes.

The spacing between major peaks still, however, corresponds to around the expected value of 4.9 eV, illustrating that the traditional textbook explanation probably suffices, if this is all the information that is required from the Franck–Hertz experiment. Otherwise, investigation of detailed spatial structures is a major task.

4. Conclusion

We have revisited the Franck–Hertz experiment and idealized it as a type of steady-state Townsend experiment, with emphasis on the kinetic theory point of view. We have related the periodic features in the observed collector current versus voltage curve to the spatial structure of electrons in gases. We have pointed out that there is a large, diverse literature associated with such periodic non-equilibrium phenomena, going back many years. In the usual textbook arguments, elastic collisions are neglected. Likewise, it is traditional to ignore or at best gloss over the importance of the velocity distribution function when analysing the Franck–Hertz experiment, or to simply assume that it is a Maxwellian. We have shown that these simplifications are justifiable when one is concerned only with the 'wavelength' of the periodic structure. If the complete spatial profile is required, the full effect of elastic collisions must be considered and there is no alternative to solving Boltzmann's equation for the phase space distribution function. In this paper, this has been carried out using a Burnett function expansion in velocity space, with no restrictions on the number of spherical harmonics in velocity space. Spatial variations have been treated in two ways, through:

(a) an eigenfunction expansion, with analysis of the real and imaginary parts of the lowest non-zero eigenvalue;
(b) finite-difference techniques.

The former technique is most suitable for dealing with the asymptotic region far downstream from the source, while the latter is essential for a description over the whole downstream region, including the near-source regime. We have considered both a model gas as well as mercury gas used in the original Franck–Hertz experiment.

Although our work fairly comprehensively analyses the *idealized* Franck–Hertz experiment, with a uniform field and in infinite space, it remains an outstanding problem to carry out such an analysis for the *actual* experiment, for which the non-uniform field as shown in figure 1 must be taken into account.

Acknowledgments

The support of the Australian Research Council is gratefully acknowledged. One author (RER) gratefully acknowledges the support of the Alexander von Humboldt Foundation, and stimulating discussions with Professors G F Hanne, R Winkler and their colleagues during the early months of 1997. The same author would also like to dedicate his contribution to the

memory of Mrs Linda Parkes, whose encouragement and support at a critical time made this paper possible.

References

[1] Franck J and Hertz G 1914 *Verh. Deutsche Phys. Ges.* **16** 457
[2] Hanne G F 1988 *Am. J. Phys.* **56** 696
[3] McMahon D R A 1983 *Am. J. Phys.* **51** 1086
[4] England J P and Elford M T 1991 *Aust. J. Phys.* **44** 647
[5] Fletcher J 1985 *J. Phys. D: Appl. Phys.* **18** 221
[6] Holst G and Oosterhuis E 1921 *Physica* **1** 78
[7] Druyvesteyn M J 1932 *Z. Phys.* **73** 33
[8] Chanin L M and Rork G D 1963 *Phys. Rev.* **132** 2547
Chanin L M and Rork G D 1964 *Phys. Rev.* **133** A1005
[9] Sakai Y, Tagashira H and Sakamoto S 1972 *J. Phys. B: At. Mol. Phys.* **5** 1010
[10] Sugawara H, Sakai Y and Tagashira H 1992 *J. Phys. D: Appl. Phys.* **25** 1483
[11] Segur P *et al* 1995 *Plasma Sources Sci. Technol.* **4** 183
[12] Winkler R *et al* 1996 *Pure Appl. Chem.* **68** 1065
Winkler R *et al* 1997 *Plasma Sources Sci. Technol.* **6** 118
[13] Sigeneger F and Winkler R 1997 *Plasma Chem. Plasma Process.* **17** 1
[14] Petrov G and Winkler R 1997 *J. Phys. D: Appl. Phys.* **30** 53
[15] Marode E and Boeuf J P 1983 *Topical Invited Lecture XVI ICPIG (Dusseldorf)* p 206
[16] Tsendin L D 1995 *Plasma Sources Sci. Technol.* **4** 200
[17] Kortshagen U, Busch C and Tsendin L D 1996 *Plasma Sources Sci. Technol.* **5** 1
[18] Robson R E 1997 Eigenvalue problems in gaseous electronics theory *Gaseous Electronics and its Applications* ed R W Crompton *et al* (Dordrecht: Kluwer) pp 89–101
[19] Date H, Kondo K, Yachi S and Tagashira H 1992 *J. Phys. D: Appl. Phys.* **25** 1330
[20] Li B 1999 *PhD Thesis* James Cook University
[21] Kumar K, Skullerud H R and Robson R E 1980 *Aust. J. Phys.* **33** 343
[22] Robson R E and Ness K F 1986 *Phys. Rev.* A **33** 2068
Ness K F and Robson R E 1986 *Phys. Rev.* A **34** 2185
[23] Mason E A and McDaniel E W 1988 *Transport Theory of Ions in Gases* (New York: Wiley)
[24] Marshak R E 1947 *Phys. Rev.* **71** 443